Desalination and Water Treatment
www.deswater.com
doi: 10.5004/dwt.2023.29929

310 (2023) 43–49
October

Ceramic membrane applied to seawater pre-treatment: effect of flocculation and temperature on microfiltration

Lorenna Alves Xavier[a], Giuliana Varela Garcia Lesak[a], Thamayne Valadares de Oliveira[b], Daniel Eiras[a], Fernando Augusto Pedersen Voll[a], Rafael Bruno Vieira[b,*]

[a]*Department of Chemical Engineering, Graduate Program in Chemical Engineering, Federal University of Paraná, CEP 81531-980 Curitiba, PR, Brazil*
[b]*Faculty of Chemical Engineering, Federal University of Uberlândia, CEP 38408-144, Uberlândia, MG, Brazil, email: rafael.bruno@ufu.br (R.B. Vieira)*

Received 17 May 2023; Accepted 30 August 2023

ABSTRACT

Microfiltration pretreatment in seawater reverse osmosis plants is essential for successful operation, as it provides high quality water for the reverse osmosis membranes. To maximize rejection during the pretreatment, coagulation–flocculation associated with ceramic microfiltration membranes was used in this work. Ferrous sulfate and anionic polyacrylamide were studied as flocculants in different temperatures in microfiltration separation using ceramic membranes. Pozzolanic clays and slag were used to prepare the ceramic membranes by uniaxial dry pressing. An increase in the hydraulic permeability from 3,982 to 11,600 $L \cdot m^{-2} \cdot h^{-1} \cdot bar^{-1}$ was obtained when the temperature increased from 20°C to 60°C. The zeta potential was close to zero with increasing temperature using flocculants. In general, the use of flocculant improved the pre-treatment of seawater by microfiltration, providing considerably higher permeated fluxes. Membrane fouling was reduced when ferrous sulfate and polyacrylamide were used at 40°C. Finally, this hybrid process at different temperatures demonstrated a significant improvement in microfiltration.

Keywords: Membrane; Flocculant; Floc size; Temperature conditions; Seawater

1. Introduction

In seawater desalination processes, membrane pretreatment has demonstrated to be an important factor for the optimization of reverse osmosis technology [1]. Pretreatment by microfiltration membranes can increase the efficiency of the seawater desalination by minimizing fouling of reverse osmosis membranes. Fouling is generated by organic and inorganic substances, particulates and colloidal matter, solid wastes and dissolved salts present in seawater [2,3]. High consumption of cleaning chemicals and decreased membrane productivity are the main problems generated by fouling [4].

Conventional processes such as coagulation/flocculation and membrane technologies (microfiltration and ultrafiltration) are the most commonly used as pretreatment for desalination [2]. Different studies have indicated that microfiltration membranes coupled with flocculation, can improve the permeate flux, and the water quality for different processes such as: microalgae separation [5] and desalination [6,7]. Yang and Kim [7] observed that the flux decline decreases with the application of coagulation before microfiltration, compared to microfiltration without flocculant. Lee et al. [8] showed that flocculation reduced the turbidity, and fouling of the microfiltration membranes. Therefore, the ability flocculation to reduce fouling of microfiltration membranes, and the turbidity of seawater is important in desalination processes.

* Corresponding author.

The temperature at which microfiltration is performed is of great importance, significantly altering membrane performance, membrane fouling, and process flux.

Currently, low-cost membranes using waste materials and clay are widely investigated [9–15]. However, pretreatment of seawater using membranes with waste materials has been scarcely studied. In our previous research [16], ceramic membrane using slag from the industrial residue, achieved good mechanical and thermal resistance, a high permeate flux, and reduced turbidity.

Numerous flocculants with aluminum-based salts or iron-based salts, anionic polyacrylamide, and Tanfloc are used for water treatment [17–22]. However, the effect of flocculants such as iron sulfate with aid anionic polyacrylamide, at different temperatures, in reducing fouling of ceramic membranes has not been documented.

Ceramic membrane systems combined with coagulation–flocculation at different temperatures has not been reported so far in desalination. In this context, the objective of this study was to investigate the use of ferrous sulfate or/and anionic polyacrylamide as coagulant–flocculant during microfiltration of seawater at different temperatures. Treatment efficiencies were assessed by measuring the permeate flux, normalized flux, zeta potential and floc size.

2. Materials and methods

2.1. Materials

2.1.1. Seawater

Seawater from Pontal do Sul, Paraná, Brazil was used in this study. The pH value, conductivity and turbidity were 8.04, 39.86 mS/cm and 3,471 NTU, respectively.

2.1.2. Membrane

Flat membranes were prepared from thermally treated clay and slag (20 wt.% slag and sintering temperatures of 1,150°C) according to Xavier et al. [16]. These membranes were analyzed by scanning electron microscopy, X-ray diffractometer, X-ray fluorescence, thermogravimetric analysis, Fourier-transform infrared spectroscopy, flexural strength, atomic force microscopy, apparent porosity and contact angle as described in the work by Xavier et al. [16]. Table 1 summarizes the properties of the prepared membrane.

2.1.3. Flocculants

A stock solution of 5 g·L^{-1} of ferrous sulfate $FeSO_4$ was used as flocculant. Anionic polyacrylamide supplied by Politécnica Química Ltda., (Brazil) was chosen as flocculant additive and it was applied as a stock solution of 1 g·L^{-1} of anionic polyacrylamide.

2.2. Experimental set-up

2.2.1. Flocculation experiment at different temperatures

Different concentrations of flocculants (Table 2) were added into seawater samples following the procedure reported in our previous paper [5] with some modifications.

Table 1
Characteristics of the fabricated membrane according to Xavier et al. [16]

Properties	Value
Main crystalline phase	Anorthite
Porosity	33.94%
Mechanical strength	16.24 MPa
Hydraulic permeability	5,263 kg·m^{-2}·h^{-1}·bar^{-1}
Thickness	2 mm
Diameter	40 mm

Table 2
Flocculation/microfiltration experiments

Run	Ferrous sulfate (g·L^{-1})	Anionic polyacrylamide (g·L^{-1})	Temperature (°C)
1	0.08	–	20
2	0.08	–	60
3	0.12	–	20
4	0.16	–	20
5	0.20	–	40
6	0.40	–	20
7	0.16	–	40
8	0.16	–	60
9	0.16	0.02	40
10	0.16	0.02	20

A thermostatic water bath was used to adjust the temperature. The samples were rapidly mixed at 100 rpm for 2 min, and then speed was reduced for 50 rpm and the mixing process continued for 5 min until flocculation was observed, after which aggregates were decanted for 10 min. Afterwards, the flocs were removed and measured. The experiments were made in duplicate.

Individual flocculation was used to define the optimal flocculant dose. In the combined process, ferrous sulfate was added at a fixed concentration of 0.16 g·L^{-1} into seawater in a mixture with anionic polyacrylamide during the rapid mixing stage (100 rpm).

2.2.2. Experimental apparatus

A schematic representation of the flocculation/microfiltration process is presented in Fig. 1.

Flocculation/microfiltration experiments were carried out at a constant flow rate of 6.94×10^{-5} m^{-3}·s^{-1} and different temperatures (20°C, 40°C, and 60°C) in a disk membrane module with an effective filtration system previously described by Nishimura et al. [5].

2.2.3. Pure water flux measurements

Initially, the membrane was compacted with deionized water at a pressure of 1.0 bar for 30 min to evaluate the uniformity in the permeate flux rate. After compaction, the

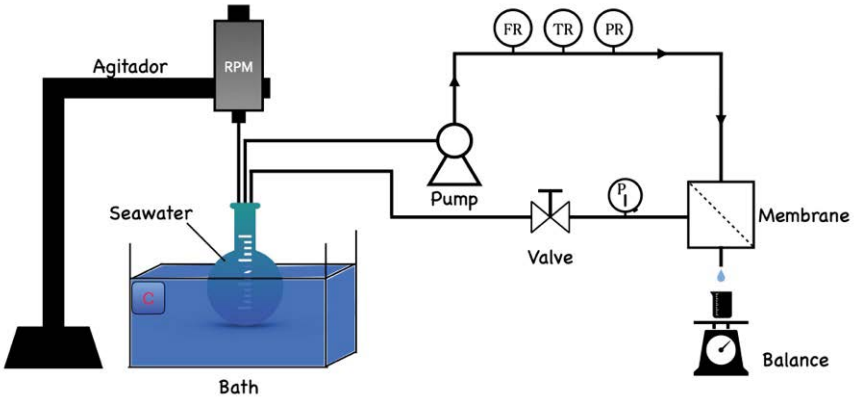

Fig. 1. Schematic representation of flocculation/microfiltration system used in this work.

permeate flux (J) were calculated with Eq. (1). The experiments were made in duplicate.

$$J = \frac{V_p}{A_p \cdot t} \tag{1}$$

where V_p is the volume of the permeate (L), A_p is the membrane area (m^2) and t is the time (s).

The hydraulic permeability L_p ($L \cdot m^{-2} \cdot h^{-1} \cdot bar^{-1}$) was evaluated at different pressures of 0.2, 0.4, 0.6, 0.8 and 1.0 bar, according to Eq. (2).

$$J = L_p \cdot \Delta P \tag{2}$$

where J is the permeate flux and ΔP the transmembrane pressure.

The resistances to permeation were calculated according to Darcy's law by Eq. (3).

$$R = \frac{\Delta P}{\mu \cdot J} \tag{3}$$

where R is the total resistance (m^{-1}), μ is the viscosity of water at 20°C, 40°C and 60°C (m·Pa·s), and ΔP (Pa) and flux ($m^3 \cdot m^{-2} \cdot s^{-1}$).

2.2.4. Flocculation coupled with microfiltration

The seawater flux through the ceramic membranes, with or without flocculant, was evaluated at a 1.0 bar for 45 min and calculated according to Eq. (1). The experiments were made in duplicate.

2.2.5. Membrane pore blocking models

To describe the pore blocking mechanism in microfiltration process, four pore blocking models were applied. Fitting of Hermia's model to evaluate the flux decline in crossflow microfiltration results in the following general Eqs. (4) and (5).

$$-\frac{dJ_V}{dt} J_V^{n-2} = k\left(J_V - J_{SS}\right) \tag{4}$$

$$-\frac{1}{A^2 J_V^3} \frac{dJ_V}{dt} = k\left(\frac{1}{AJ_V}\right)^n \tag{5}$$

where J_{SS}, J_V, A, n and k are respectively: steady state flux, permeate flux, filtration area, pore blocking index and a constant. The blocking mechanisms are classified as: complete (n = 2), standard (n = 1.5), intermediate (n = 1), and cake filtration (n = 0). To minimize the objective function, Scilab's *fminsearch* function was used according to Lesak et al. [11].

2.3. Analysis

The zeta potential and floc size were analyzed by the Zetasizer nano instrument (Nano ZS90). The samples were diluted 20 times, the analyses were made in triplicates.

3. Results and discussion

3.1. Characterization of microfiltration

3.1.1. Influence of the temperature on hydraulic permeability

The pure water flux through ceramic membrane was investigated at temperatures of 20°C, 40°C and 60°C and the results are shown in Fig. 2. The water flux increased linearly with the applied pressure. This trend is predicted by Darcy's law given in Eq. (2).

The obtained value of L_p for the membrane at 20°C, 40°C, and 60°C, are 3,982; 5,714 and 11,600 $L \cdot m^{-2} \cdot h^{-1} \cdot bar^{-1}$, respectively, which suggests that the permeate flux increases linearly with feed temperature. This behavior indicates that higher feed temperature leads to a lower feed viscosity, decrease of concentration polarization and the solvent transport through the membrane is intensified, resulting in a higher permeate flux [23].

Similar observation was reported by other researchers regarding the use of ceramic membrane. Lesak et al. [11] worked with disk-type ceramic membranes made of Pristine modified clay and clay mixed with niobium pentoxide (Nb–1100), obtaining permeabilities of 0.793 × 10^{-6} to 3.498 × 10^{-6} $kg \cdot m^{-2} \cdot s^{-1} \cdot Pa$, respectively. Mouiya et al. [24] developed microfiltration ceramic membrane to evaluate the

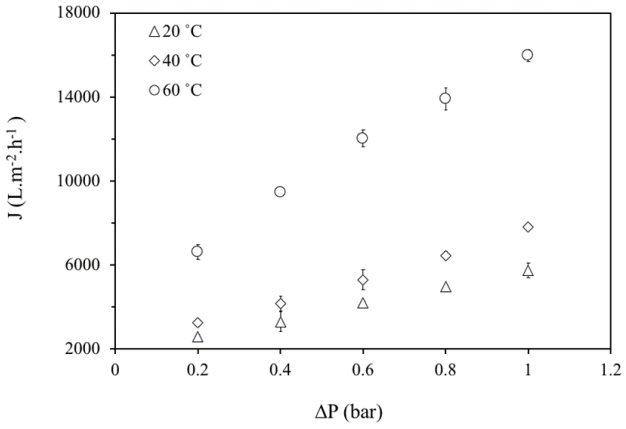

Fig. 2. Permeate flux at 20°C, 40°C and 60°C.

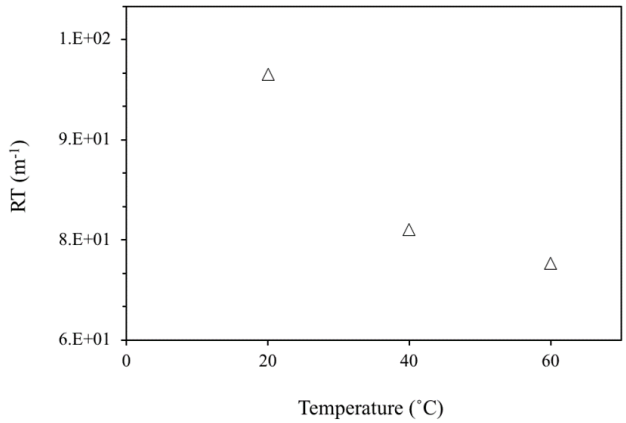

Fig. 3. Total resistance at different temperatures.

pre-treatment of seawater desalination, obtaining a water permeability of value of 928 $L \cdot h^{-1} \cdot m^{-2} \cdot bar^{-1}$. Therefore, the hydraulic permeabilities obtained in this work are within the values reported in the literature for other disk-type ceramic membranes, and, especially for 60°C, the permeability value was relatively high.

The water flux increases more than three times with the increase in feed temperature from 20°C to 60°C. Similar temperature dependence on permeate flux was reported by Goosen et al. [25], increasing the temperature of 20°C to 40°C. According to them, the permeate flux increased from 12.4 to 24.1 $L \cdot m^{-2} \cdot h^{-1} \cdot bar^{-1}$ when the feed temperature was increased from 30°C to 40°C.

Fig. 3 shows that higher temperature reduces the total resistance (RT) due to the higher solubility of the water.

As shown in Fig. 3, RT decreases considerably when the temperature increases to 40°C, but further increases in temperature, do not decrease RT which remains constant at 60°C. Therefore, considering the higher operating costs at higher temperatures it is recommended to operate the process at 40°C.

3.1.2. Flocculation and microfiltration at different feed temperatures

The permeate flux of the feed solution was evaluated at 20°C, 40°C and 60°C with the addition of the flocculants. Fig. 4 shows the evolution of permeate flux with time. Results are shown for ten runs according to Table 1.

The permeate flux increased with increasing temperature. Thus, the temperature and filtration time had a considerable influence on the permeation flux.

The permeate flux measured at 20°C increased and then stabilized with the increase of ferrous sulfate concentration. The highest fluxes at 20°C were 1,058; 1,178; 1,687 and 1,618 $L \cdot h^{-1} \cdot m^{-2}$, respectively, which were achieved at ferrous sulfate concentrations of 0.08, 0.12, 0.16 and 0.40 $g \cdot L^{-1}$. The amount of ferrous sulfate required to obtain the maximum flux was 0.16 $g \cdot L^{-1}$. The initial flux in the first 5 min was 1,336 $L \cdot m^{-2} \cdot h^{-1}$ for the run with a concentration of ferrous sulfate of 0.16 $g \cdot L^{-1}$ at 20°C. The flux gradually decreased to 819 $L \cdot m^{-2} \cdot h^{-1}$ after 30 min before reaching a stable value. This value for the permeate flux was lower than the flux

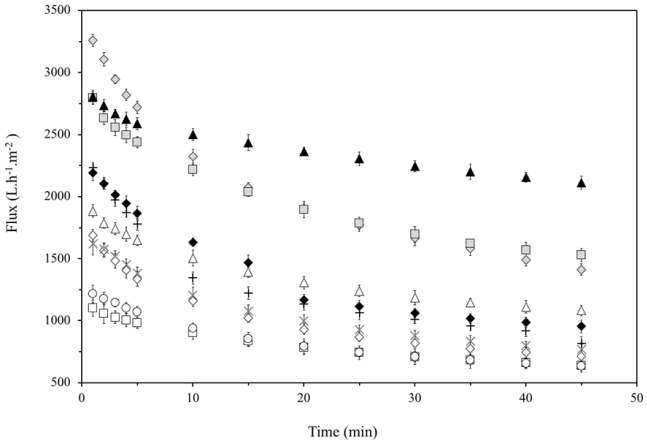

Fig. 4. Evolution of permeate flux with time with different flocculants and at different temperatures. (×) FS 0.40 $g \cdot L^{-1}$ 20°C, (◇) FS 0.16 $g \cdot L^{-1}$ 20°C, (○) FS 0.12 $g \cdot L^{-1}$ 20°C, (□) FS 0.08 $g \cdot L^{-1}$ 20°C, (△) FS 0.16 $g \cdot L^{-1}$ + AP 0.02 $g \cdot L^{-1}$ 20°C, (+) FS 0.20 $g \cdot L^{-1}$ 40°C, (◆) FS 0.16 $g \cdot L^{-1}$ 40°C, (▲) FS 0.16 $g \cdot L^{-1}$ + AP 0.02 $g \cdot L^{-1}$ 40°C, (◈) FS 0.16 $g \cdot L^{-1}$ 60°C and (▣) FS 0.08 $g \cdot L^{-1}$ 60°C.

obtained for the same membrane and pressure using raw seawater (without flocculant) from the same batch, which started with an initial flux of 1,559 $L \cdot m^{-2} \cdot h^{-1}$ and after 30 min of filtration, decreased to 952 $L \cdot m^{-2} \cdot h^{-1}$. This behavior could be explained by fouling due to the interaction between the membrane and the flocculants. Studies have reported that flocculation pre-treatment can affect filtration, and flocculant dosage is an important factor [26,27].

Moreover, it is possible to verify in Fig. 4 that at 40°C the concentration of ferrous sulfate (0.16 and 0.20 $g \cdot L^{-1}$) does not affect the initial and final permeate fluxes. However, at 0.16 $g \cdot L^{-1}$ of ferrous sulfate, in the first 10 and 15 min the permeate flux was higher than that of ferrous sulfate of 0.20 $g \cdot L^{-1}$. In contrast, at 60°C for ferrous sulfate, as the concentration was increased from 0.08 to 0.16 $g \cdot L^{-1}$, the flux constantly increased from 2,794 to 3,259 $L \cdot m^{-2} \cdot h^{-1}$.

The variations in flux at various ferrous sulfate concentrations are probably associated with floc formation at different temperatures (20°C, 40°C and 60°C). Flocs can

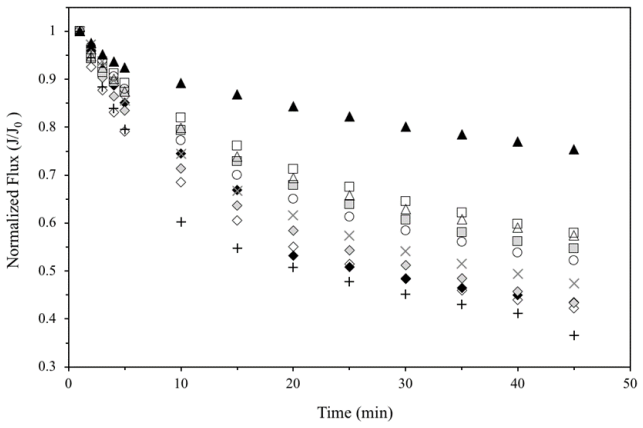

Fig. 5. Normalized permeate flux as a function of the microfiltration duration. (×) FS 0.40 g·L^{-1} 20°C, (◇) FS 0.16 g·L^{-1} 20°C, (○) FS 0.12 g·L^{-1} 20°C, (□) FS 0.08 g·L^{-1} 20°C, (△) FS 0.16 g·L^{-1} + AP 0.02 g·L^{-1} 20°C, (+) FS 0.20 g·L^{-1} 40°C, (◆) FS 0.16 g·L^{-1} 40°C, (▲) FS 0.16 g·L^{-1} + AP 0.02 g·L^{-1} 40°C, (◈) FS 0.16 g·L^{-1} 60°C and (■) FS 0.08 g·L^{-1} 60°C.

promote membrane resistance reduction and improve the membrane flux [5,26]. In this study, increasing the temperature from 20°C to 40°C with the concentration of ferrous sulfate of 0.16 g·L^{-1}, led to an increase of the permeate flux from 1,688 to 2,192 L·h^{-1}·m^{-2}.

The optimal concentration of ferrous sulfate was 0.16 g·L^{-1}. The use of anionic polyacrylamide (0.02 g·L^{-1}) increased the permeate flux at 20°C and 40°C, compared to the permeate flux obtained with the coagulant alone at the same temperature condition. In general, permeation fluxes reached a stable value within 45 min of filtration.

The trends of normalized permeate flux vs. time are depicted in Fig. 5.

As can be seen, double flocculation of ferrous sulfate + polyacrylamide at 40°C decreased membrane fouling, reflecting in higher permeate fluxes. Using polyacrylamide, the normalized flux was more stable during the first 45 min (from 1.1 to 0.75). The phenomenon was attributed to the formation, and accumulation of large flocs on the membrane surface which retained the small particles and increased the permeated flux.

Johir et al. [6] evaluated the performance of flocculation in line with filtration as a pre-treatment for reverse osmosis desalination. They used $FeCl_3$ as flocculant and obtained a normalized flux decline (J/J_0) from 0.35 to 0.22 during the first 20 h.

3.2. Pore blocking models

The fouling mechanisms were studied for the microfiltration of seawater flocculated. Table 3 presents the parameters evaluated from the fitted pore blocking models.

The best fitting models were complete and intermediate pore blocking mechanism ($R^2 > 0.98$), and cake formation ($R^2 > 0.97$).

For the following studies, a complete pore blocking adjusted coefficient (k_c) was plotted vs. temperature (Fig. 6)

Table 3
Results of the parameters of the models

Model	Complete	Standard	Intermediate	Cake filtration
	FS 0.16 g·L^{-1} 20°C			
R^2	0.994	0.93	0.996	0.992
K	5.303	1.221	0.004	3.43E-06
	FS 0.16 g·L^{-1} 40°C			
R^2	0.993	0.997	0.986	0.975
K	4.621	0.998	0.003	1.70E-06
	FS 0.16 g·L^{-1} 60°C			
R^2	0.996	0.978	0.996	0.99
K	4.499	0.787	0.002	7.60E-07
	FS 0.08 g·L^{-1} 20°C			
R^2	0.994	0.982	0.991	0.986
K	3.911	0.789	0.004	4.85E-06
	FS 0.08 g·L^{-1} 60°C			
R^2	0.993	0.979	0.99	0.984
K	4.279	0.577	0.002	8.65E-07
	FS 0.12 g·L^{-1} 20°C			
R^2	0.998	0.974	0.996	0.991
K	4.296	0.958	0.004	4.63E-06
	FS 0.20 g·L^{-1} 40°C			
R^2	0.995	0.949	0.996	0.991
K	6.014	1.233	0.004	2.22E-06
	FS 0.40 g·L^{-1} 20°C			
R^2	0.998	0.976	0.996	0.99
K	4.362	0.975	0.004	2.81E-06
	FS 0.16 g·L^{-1} + AP 0.02 g·L^{-1} 20°C			
R^2	0.994	0.971	0.993	0.989
K	4.383	0.643	0.003	1.89E-06
	FS 0.16 g·L^{-1} + AP 0.02 g·L^{-1} 40°C			
R^2	0.98	0.966	0.98	0.979
K	3.712	0.234	0.001	5.96E-07

to evaluate the effect of temperature on membrane fouling. In this case, a mixture containing 0.16 g·L^{-1} of ferrous sulfate and 0.02 g·L^{-1} of anionic polyacrylamide was used as flocculant. It can be observed that complete pore blocking coefficient k_c decreases when temperature is increased (20°C, 40°C and 60°C). Furthermore, the anionic polyacrylamide induced the reduction of k_c from 4.383 to 3.712 at 20°C and 40°C, respectively. This result is consistent with the observation that the increase in temperature up to 40°C improves the flux and reduces membrane fouling.

The increase in temperature can enlarge membrane pore size, reducing the probability of deposition on membrane surface and complete pore blocking [28].

3.3. Flocculation performance

3.3.1. Zeta potential

Fig. 7 shows the zeta potential of seawater without flocculant and seawater flocculated as a function of temperature. In the absence of flocculant, the increase in temperature up to 40°C decreases the zeta potential of seawater from −2.55 to −8 mV, indicating high salinity and the presence of dissolved materials in seawater. These results are in good agreement with previous studies, where the zeta potential of seawater became more negative as seawater was diluted, which can be attributed to dissolution of ions at different temperatures [19].

The zeta potential shows positive values for samples with ferrous sulfate and anionic polyacrylamide. In the presence of flocculants, the zeta potential decreased with increasing temperature. However, the decrease was higher with dual flocculation (ferrous sulfate and anionic polyacrylamide). As shown in Fig. 7, the zeta potential was reduced from 7.05 to 0.18 mV as the temperature increased from 20°C to 60°C. The repulsive forces between the particles decrease as the zeta potential approaches zero, which facilitates agglomeration of the particles [29].

These results show that the influence of temperature and the type of flocculant influence particle agglomeration due to interactions between the negatively charged groups of the polyacrylamide and the salt ions present in seawater [30].

3.3.2. Floc size

Fig. 8 shows the results obtained for ferrous sulfate (0.16 g·L^{-1}), and anionic polyacrylamide (0.02 g·L^{-1}). Before flocculation, particle size in the seawater was smaller. Therefore, the increase in the floc size (regardless of temperature) due to the addition of ferrous sulfate affected membrane fouling.

The addition of anionic polyacrylamide increased floc size with the increase in temperature. The higher floc size was obtained at 60°C, followed by 40°C and 20°C. These results are consistent with previous findings showing that anionic polyacrylamide properties lead to enhanced aggregating power and formation of larger and denser flocs due to bridging [31]. Therefore, the floc size should be considered as a new control parameter in flocculation and microfiltration coupled systems.

4. Conclusion

In this work, flocculation and microfiltration membrane process was studied, as pre-treatment for seawater, and the effect of flocculants and temperature on the reduction of fouling was evaluated. The performance of the coupled process showed a significant improvement in the permeate flux, when compared to direct microfiltration. The filtration of seawater using ferrous sulfate and anionic polyacrylamide through the membrane at 40°C, showed a better performance in terms of fouling reduction, permeate flux and normalized flux. This could be attributed to particle aggregation with the help of flocculant and temperature, leading to the formation of larger and denser flocs. The characterization of the flocculation by the zeta potential and floc size techniques confirms the efficiency of the flocculation at different temperatures (20°C, 40°C and 60°C). Flocculation of seawater at 60°C leads to an increase in the floc size and zeta potential approached zero. Therefore, taking in consideration the constant permeate flux, normalized flux and fouling mechanism, the combination of these

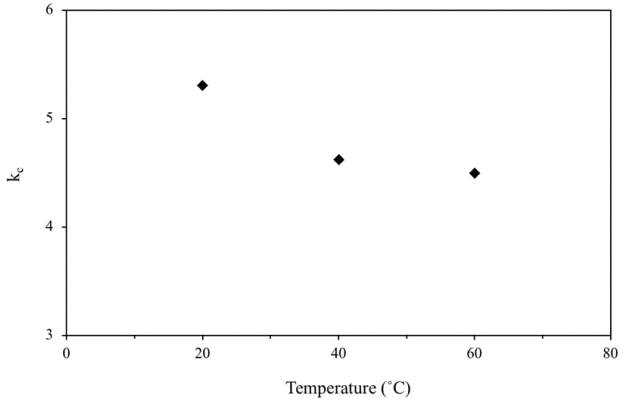

Fig. 6. Complete pore blocking adjusted coefficient (k_c) vs. temperature.

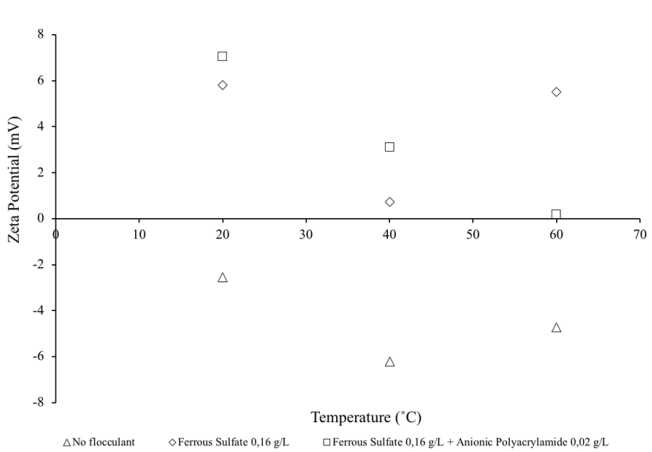

Fig. 7. Effect of temperature and flocculants on zeta potential.

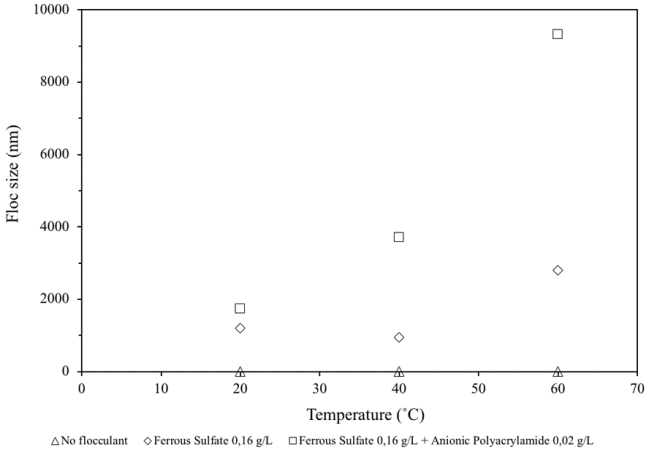

Fig. 8. Effect of temperature and flocculants on floc size.

processes using ferrous sulfate (0.16 g·L^{-1}) and anionic polyacrylamide (0.02 g·L^{-1}) at 40°C has a greater potential for pre-treatment of seawater.

Acknowledgements

This work was supported by the Brazilian National Council of Scientific and Technological Development (CNPq) [Grant Number 425125/2018-1 and 454669/2014-3] and by CAPES. The authors thank the Federal University of Paraná for infrastructural support.

The authors have declared no conflict of interest.

References

[1] A. Belgada, B. Achiou, S. Alami Younssi, F.Z. Charik, M. Ouammou, J.A. Cody, R. Benhida, K. Khaless, Low-cost ceramic microfiltration membrane made from natural phosphate for pretreatment of raw seawater for desalination, J. Eur. Ceram. Soc., 41 (2021) 1613–1621.
[2] D.A.R.O. da Silva, L.C.B. Zuge, A. de Paula Scheer, Pretreatments for seawater desalination by pervaporation using the developed green silica/PVA membrane, J. Environ. Chem. Eng., 9 (2021) 106327, doi: 10.1016/j.jece.2021.106327.
[3] S. Jeong, S. Vigneswaran, Assessment of biological activity in contact flocculation filtration used as a pretreatment in seawater desalination, Chem. Eng. J., 228 (2013) 976–983.
[4] S.T. Mitrouli, S.G. Yiantsios, A.J. Karabelas, M. Mitrakas, M. Føllesdal, P.A. Kjolseth, Pretreatment for desalination of seawater from an open intake by dual-media filtration: pilot testing and comparison of two different media, Desalination, 222 (2008) 24–37.
[5] T. Nishimura, G.V. Garcia Lesak, L. Alves Xavier, R. Bruno Vieira, A. Bellin Mariano, Effects of flocculant concentration and temperature on the membrane separation process in microalgal suspensions, Chem. Eng. Technol., 45 (2022) 230–237.
[6] A.H. Johir, C. Khorshed, S. Vigneswaran, H.K. Shon, In-line flocculation–filtration as pre-treatment to reverse osmosis desalination, Desalination, 247 (2009) 85–93.
[7] H.-J. Yang, H.-S. Kim, Effect of coagulation on MF/UF for removal of particles as a pretreatment in seawater desalination, Desalination, 247 (2009) 45–52.
[8] J.J. Lee, M.A.H. Johir, K.H. Chinu, H.K. Shon, S. Vigneswaran, J. Kandasamy, C.W. Kim, K. Shaw, Hybrid filtration method for pre-treatment of seawater reverse osmosis (SWRO), Desalination, 247 (2009) 15–24.
[9] B. Achiou, H. Elomari, A. Bouazizi, A. Karim, M. Ouammou, A. Albizane, J. Bennazha, S. Alami Younssi, I.E. El Amrani, Manufacturing of tubular ceramic microfiltration membrane based on natural pozzolan for pretreatment of seawater desalination, Desalination, 419 (2017) 181–187.
[10] I. Jedidi, S. Saïdi, S. Khemakhem, A. Larbot, N. Elloumi-Ammar, A. Fourati, A. Charfi, A. Ben Salah, R. Ben Amar, Elaboration of new ceramic microfiltration membranes from mineral coal fly ash applied to waste water treatment, J. Hazard. Mater., 172 (2009) 152–158.
[11] G.V.G. Lesak, L.A. Xavier, T.V. de Oliveira, E. Fontana, A.F. Santos, V.L. Cardoso, R.B. Vieira, Enhancement of pozzolanic clay ceramic membrane properties by niobium pentoxide and titanium dioxide addition: characterization and application in oil-in-water emulsion microfiltration, J. Pet. Sci. Eng., 217 (2022) 110892, doi: 10.1016/j.petrol.2022.110892.
[12] W. de Melo, G.V.G. Lesak, T.V. de Oliveira, F.A.P. Voll, A.F. Santos, R.B. Vieira, Microfiltration of oil-in-water emulsion using modified ceramic membrane: surface properties, membrane resistance, critical flux, and cake behavior, Mater. Res., 25 (2022), doi: 10.1590/1980-5373-mr-2021-0365.
[13] J.D. de O. Henriques, M.W. Pedrassani, W. Klitzke, T.V. de Oliveira, P.A. Vieira, A.B. Mariano, R.B. Vieira, Fabrication and characterization of low cost ceramic membranes for microfiltration of *Acutodesmus obliquus* using modified clays, Matéria (Rio Janeiro), 24 (2019), doi: 10.1590/s1517-707620190004.0826.
[14] J.D. de O. Henriques, M.W. Pedrassani, W. Klitzke, A.B. Mariano, J.V.C. Vargas, R.B. Vieira, Thermal treatment of clay-based ceramic membranes for microfiltration of *Acutodesmus obliquus*, Appl. Clay Sci., 150 (2017) 217–224.
[15] A. Mendes, D.J. de Oliveira, T. de Oliveira, V.F.A. Pederson, R. Vieira, A. Mariano, Effects of microalgal concentration and pH with flocculant on microfiltration, Chem. Ind. Chem. Eng. Q., 29 (2023) 253–262.
[16] L.A. Xavier, D.E.L. Fetzer, T.V. de Oliveira, D. Eiras, F.A.P. Voll, R.B. Vieira, Effect of stainless-steel slag concentration in the fabrication of cost-effective ceramic membranes: seawater pre-treatment application, Ceram. Int., 48 (2022) 23273–23283.
[17] S. Jeong, F. Nateghi, T.V. Nguyen, S. Vigneswaran, A.T. Tuan, Pretreatment for seawater desalination by flocculation: performance of modified poly ferric silicate (PFSi-δ) and ferric chloride as flocculants, Desalination, 283 (2011) 106–110.
[18] R.I. Jeldres, M. Jeldres, M.R. MacIver, M. Pawlik, P. Robles, N. Toro, Analysis of kaolin flocculation in seawater by optical backscattering measurements: effect of flocculant management and liquor conditions, Minerals, 10 (2020) 317, doi: 10.3390/min10040317.
[19] P. Mpofu, J. Addai-Mensah, J. Ralston, Temperature influence of nonionic polyethylene oxide and anionic polyacrylamide on flocculation and dewatering behavior of kaolinite dispersions, J. Colloid Interface Sci., 271 (2004) 145–156.
[20] R.H.R. Hanashiro, C.B. Stoco, T.V. de Oliveira, M.K. Lenzi, A.B. Mariano, R.B. Vieira, Experimental validation of hindered settling models and flux theory applied in continuous flow process for harvesting *Acutodesmus obliquus*, Can. J. Chem. Eng., 97 (2019) 1903–1912.
[21] A. Shrestha, G. Naidu, M.A.H. Johir, J. Kandasamy, S. Vigneswaran, Performance of flocculation titanium salts for seawater reverse osmosis pretreatment, Desal. Water Treat., 98 (2017) 92–97.
[22] J. Duan, A. Niu, D. Shi, F. Wilson, N.J.D. Graham, Factors affecting the coagulation of seawater by ferric chloride, Desal. Water Treat., 11 (2009) 173–183.
[23] J. Xu, C.Y. Chang, C. Gao, Performance of a ceramic ultrafiltration membrane system in pretreatment to seawater desalination, Sep. Purif. Technol., 75 (2010) 165–173.
[24] M. Mouiya, A. Abourriche, A. Bouazizi, A. Benhammou, Y. El Hafiane, Y. Abouliatim, L. Nibou, M. Oumam, M. Ouammou, A. Smith, H. Hannache, Flat ceramic microfiltration membrane based on natural clay and Moroccan phosphate for desalination and industrial wastewater treatment, Desalination, 427 (2018) 42–50.
[25] M.F.A. Goosen, S.S. Sablani, S.S. Al-Maskari, R.H. Al-Belushi, M. Wilf, Effect of feed temperature on permeate flux and mass transfer coefficient in spiral-wound reverse osmosis systems, Desalination, 144 (2002) 367–372.
[26] R. Bergamasco, L.C. Konradt-Moraes, M.F. Vieira, M.R. Fagundes-Klen, A.M.S. Vieira, Performance of a coagulation-ultrafiltration hybrid process for water supply treatment, Chem. Eng. J., 166 (2011) 483–489.
[27] K. Konieczny, D. Sąkol, J. Płonka, M. Rajca, M. Bodzek, Coagulation—ultrafiltration system for river water treatment, Desalination, 240 (2009) 151–159.
[28] W. Zhang, L. Ding, Investigation of membrane fouling mechanisms using blocking models in the case of shear-enhanced ultrafiltration, Sep. Purif. Technol., 141 (2015) 160–169.
[29] A. Kumar, C.K. Dixit, Chapter 3 - Methods for Characterization of Nanoparticles, in: Advances in Nanomedicine for the Delivery of Therapeutic Nucleic Acids, Woodhead Publishing, 2017, pp. 43–58. Available at: https://doi.org/10.1016/B978-0-08-100557-6.00003-1
[30] Z. Amir, I.M. Said, B.M. Jan, M. Khalil, Molecular analysis on retardation on polyacrylamide in high salinity and high temperature conditions, AIP Conf. Proc., 2168 (2019) 5132488, doi: 10.1063/1.5132488.
[31] B. Bolto, J. Gregory, Organic polyelectrolytes in water treatment, Water Res., 41 (2007) 2301–2324.